

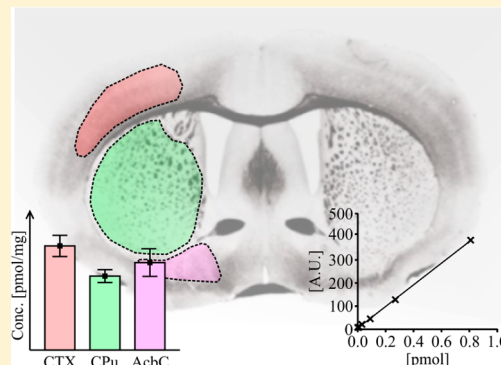
msIQuant – Quantitation Software for Mass Spectrometry Imaging Enabling Fast Access, Visualization, and Analysis of Large Data Sets

Patrik Källback, Anna Nilsson, Mohammadreza Shariatgorji, and Per E. Andrén*

Biomolecular Imaging and Proteomics, National Resource for Mass Spectrometry Imaging, Department of Pharmaceutical Biosciences, Uppsala University, Box 591, SE-75124 Uppsala, Sweden

 Supporting Information

ABSTRACT: This paper presents msIQuant, a novel instrument- and manufacturer-independent quantitative mass spectrometry imaging software suite that uses the standardized open access data format imzML. Its data processing structure enables rapid image display and the analysis of very large data sets (>50 GB) without any data reduction. In addition, msIQuant provides many tools for image visualization including multiple interpolation methods, low intensity transparency display, and image fusion. It also has a quantitation function that automatically generates calibration standard curves from series of standards that can be used to determine the concentrations of specific analytes. Regions-of-interest in a tissue section can be analyzed based on a number of quantities including the number of pixels, average intensity, standard deviation of intensity, and median and quartile intensities. Moreover, the suite's export functions enable simplified postprocessing of data and report creation. We demonstrate its potential through several applications including the quantitation of small molecules such as drugs and neurotransmitters. The msIQuant suite is a powerful tool for accessing and evaluating very large data sets, quantifying drugs and endogenous compounds in tissue areas of interest, and for processing mass spectra and images.



Matrix-assisted laser desorption ionization mass spectrometry imaging (MALDI-MSI)¹ has become a popular analytical method for directly studying multimodal molecular species including endogenous proteins,^{2,3} peptides,⁴ lipids,⁵ neurotransmitters,⁶ and small molecule pharmaceutical substances² in different types of tissue sections.^{1,7,8} Most software packages for visualizing MSI data are only designed to perform qualitative analysis. In addition, the software tools for acquiring and visualizing MSI data are usually instrument vendor specific and proprietary. To overcome these shortcomings, open access MSI data formats such as Analyze 7.5⁹ and imzML¹⁰ have been developed to ensure comparability of data collected from various types of instruments and manufacturers. Analyze 7.5 is less flexible than imzML, because it can only store data for a limited number of *m/z* channels (32,768). This is a limitation because mass spectra generated using certain instruments such as Fourier Transform Ion Cyclotron Resonance (FTICR) mass spectrometers can contain over 1,000,000 *m/z* channels; imzML can be used to store and manipulate such large data sets but Analyze 7.5 cannot. Existing software packages that can use the imzML format include BioMap,¹¹ Datacube Explorer,¹² OmniSpect,¹³ Mirion,¹⁴ MSiReader,¹⁵ and SpectViewer.¹⁶ Commercial software packages that can handle the imzML format have also been launched, such as TissueView (AB Sciex), MALDIVision (Premier Biosoft), and Quantinetix (ImaBiotech) MALDI Imaging Software.

We recently presented a novel MSI software package that features protocols for quantitation of drugs and endogenous

compounds.¹⁷ The program can be used to process predefined regions-of-interest (ROI) in a tissue section, retrieve the corresponding mass spectrometric data, and apply several different spectral processing techniques including baseline correction, baseline subtraction and denoising, spectrum smoothing, spectrum recalibration, and normalization. In this publication, it was disclosed that deuterated labeled internal standards¹⁷ can be used to compensate for signal fluctuations in mass spectrometric images of tissue sections and that this strategy makes it possible to directly image and quantitate drugs and endogenous peptides in tissue sections. The use of deuterated internal standards significantly improved the normalization of target analytes in tissue sections and increased pixel-to-pixel precision.^{17–21} This technique enabled us to perform the first quantitation of an endogenous neuropeptide directly in brain tissue sections and to quantitate drug molecules in organs such as the brain and lung.¹⁷

Unfortunately, the previously reported version of our software is limited in that it can only read data from one instrument manufacturer and requires ROI selection to be performed using that manufacturer's software. Here we present a novel quantitation software suite for MSI, msIQuant, which reads data in the imzML format and can be used to process,

Received: December 4, 2015

Accepted: March 25, 2016

Published: March 25, 2016



visualize, and quantitatively analyze data generated using mass spectrometers made by all major manufacturers of MSI instruments. The new software has several important new features including (i) the ability to load large (>50 GB) data sets within a few seconds and to analyze such data without any data reduction, (ii) spectra processing functionalities such as automatic spectra alignment, (iii) an integrated user interface for controlling the individual steps of the quantitation process and retrieving data during image processing, (iv) the ability to define different types of ROIs, (v) automatic generation of calibration standard curve for quantitation, (vi) extraction of data from ROIs for subsequent analysis, (vii) new image visualization options including interpolation, normalization, and rainbow and color scales, (viii) low intensity transparency display capabilities, (ix) a hotspot indicator, (x) intensity profile measurement for selected ions along a line in a tissue section, and (xi) a molecular image fusion option for sharpening of MSI images. We also present several illustrative applications that demonstrate the strengths of msIQuant.

MATERIAL AND METHODS

Animals and Tissue Preparation. Adult male rats (Wistar or Sprague–Dawley) and adult male mice (C57BL/6J) were used in the studies. The animals were housed in air-conditioned rooms with a 12 h dark/light cycle at 20 °C, with a humidity of 53% and food *ad libitum*. Coronal or sagittal brain tissue sections were obtained from untreated rats or mice. Rat lung tissue sections were prepared from animals administered tiotropium bromide at a dosage of 10 µg/kg by *in vivo* inhalation.²² All animals were euthanized followed by rapidly dissecting out their brain or lung tissues, freezing the tissues in dry ice-cooled isopentane, and storing them at –80 °C until further use. The studies were conducted in accordance with the European Communities Council Directives of 1986 (86/609/EEC) and 2010 (2010/63/EU) and were approved by the local ethical Committees on animal experiments.

Coronal rat and sagittal mouse brain tissue sections were cut at a thickness of 14 µm. Frozen rat lung sections were cut at a thickness of 14 µm along the long flat frontal plane of the left lobe, from side to side, to get full section of the central airways. All tissue sections were cut using a cryomicrotome (Leica CM3050S, Leica Microsystems, Germany) at a temperature of –20 °C and thaw mounted onto conductive indium tin oxide coated (ITO) slides (Bruker Daltonics, Bremen, Germany) or conventional microscope glass slides. Optical images were acquired using a standard flatbed scanner (Seiko Epson, Japan) before MALDI matrix application. MALDI matrices were applied to the tissue sections using automatic spraying devices (ImagePrep, Bruker Daltonics and TM-Sprayer, HTX Technologies LLC, Chapel Hill, NC). Two different matrices were used: α-cyano-4-hydroxycinnamic acid (CHCA; 5 mg/mL in 50% acetonitrile, 0.1% TFA) and a reactive matrix; 2,4-diphenylpyranyl tetrafluoroborate (DPP-TFB; 1.3 mg/mL in 58% methanol, 0.07% triethylamine).²³

MS Imaging. MALDI-MSI was performed using ultraflexXtreme TOF/TOF, Solarix XR 12 T (Bruker Daltonics), LTQ Orbitrap XL (Thermo Scientific, San Jose, CA, USA), and Synapt G2si (Waters Corp., Manchester, UK) instruments. Acquisitions conducted with the ultraflexXtreme and Solarix XR instruments were set up using flexControl 4.0 and flexImaging 4.0 (Bruker Daltonics), and the MALDI MSI experiments were performed in positive reflectron mode. Acquisitions conducted

with the LTQ Orbitrap XL instrument were set up using XCalibur 2.0.7 (Thermo Scientific) in positive ionization mode.

Desorption electrospray ionization (DESI)-MSI experiments were carried out using Q-TOF mass spectrometers (Synapt G2si, Waters Corp.). The instruments' DESI source (2D-DESI, Prosolia, Indianapolis, IN, USA) incorporated an electrospray probe and were utilized for imaging by rastering the sample surface under the spray using a high precision XY stage. All MSI data were acquired in V-mode, for *m/z* values of up to 1,200, in positive mode. Sodium formate was initially used as the spray solution, and its clusters were used to calibrate the instrument prior to acquisition. The DESI spray solvent used in tissue analyses was a mixture of methanol and water (98:2 v/v) and was delivered at a flow rate of 1.5–2 µL/min using a syringe pump (Model 55-2222, Harvard Apparatus, Holliston, MA). A voltage of 4.5 kV was applied to the solvent, and nitrogen was used as the nebulizing gas at 5 bar. Tissue sections were scanned in a horizontal line at a rate of 100 µm/s and rows were separated by a vertical step of 100 µm, generating an ultimate pixel size of 100 µm in ion images. MSI experiments performed on the Synapt G2si were set up using the High Definition Imaging (HDI) software (v1.3, Waters Corp.).

Software Development. Programming Language. The msIQuant executable files (.exe) and dynamic-link libraries (.dll) were written in the C++ programming language, and the complete project consists of more than 100k lines of code. The .NET Framework, version 4.0 (Microsoft Corp., Redmond, WA, USA) was used for the 2D graphics, and Microsoft Visual Studio 2010 was used as the software development environment. The executable files were compiled for 64-bit (x64) platforms to enable access to the large memory space of modern computers and to exploit the quick arithmetic capability of 64-bit central processing units (CPUs). msIQuant runs on Microsoft Windows 7 and more recent versions of this operating system.

Import of MSI Data to msIQuant. msIQuant reads MSI data in the imzML data format, which is supported through an export function by most MSI instrumentation manufacturers. This means that msIQuant is manufacturer-independent and compatible with MSI data acquired using diverse ionization techniques and mass analyzers.²⁴ The spectra and the spectra transposes of the msIQuant data format are generated from the binary component of the imzML data. By adding additional information such as tissue thickness, tissue density, and selected tissue regions, msIQuant can record all of the information required to evaluate MSI data.

The msIQuant User Views, Data Processing, and Evaluation. An integrated ease-of-use interface has been implemented containing project-, spectra-, mass list-, and image views, located in a logical order (see Supporting Information, Figure S1 and Table S1).

Data Format. An msIQuant file is divided into seven main sections: (i) the header, which contains information about the different input files, the version number, and a unique identifier number; (ii) ROI data; (iii) biological data, including information about the species, tissue type, tissue thickness, and tissue density; (iv) optical and histological images; (v) quantitation information; vi) the imzML experiment; and, finally, vii) the msIQuant spectra data, which contains information about normalization factors, spectra processing, and peak information. The msIQuant data is created from the binary component of an imzML file, which may be in one of four formats: continuous profile data, processed profiles,

continuous centroid (hypothetical) data, and processed centroid data.¹⁰ Regardless of the binary component's format, it is initially stored as a compressed continuous profile for speed of access. If the imzML data is in the continuous profile format, it is copied into the msIQuant data file without further processing. If the imzML data is in the processed profile format, an *m/z* array is created to accommodate all the data that has defined minimum and maximum *m/z* values as well as mass resolution. The processed profile data is then placed into the created *m/z* array and stored as a continuous profile in msIQuant format. The centroid binary imzML format is less readily converted into the continuous profile msIQuant format. For this purpose, an algorithm that converts the centroid data to profile data was created. This algorithm finds the minimum gap between two centroid peaks, calculates the resolution of the spectrum, and fits these two narrow peaks with Gaussian distributions and baseline separation. All of the centroid data are analyzed to find the minimum and maximum *m/z* values of the spectra; these values are then used together with the calculated resolution to create an *m/z* array. Continuous profile data is then created by fitting all of the Gaussian peaks created from the centroids into the resulting spectra. During this process, the factors of the different normalization methods are calculated for each spectrum and stored as an array in the data.

A large data set stored in the external memory may need to be reduced to fit into the internal memory unless the computer has a very large memory. For example, an FTICR MS experiment may require up to 128 GB of internal memory. These high memory requirements create problems including high investment costs and long data loading times. MSI data are therefore often reduced somehow, for instance by binning to reduce the number of *m/z* channels, cutting the beginning and end of each spectrum to reduce the number of *m/z* channels while maintaining the mass resolution, and/or reducing the imaging area (i.e., the number of pixels) loaded into the memory.

A novel approach to data handling is used to circumvent this problem in msIQuant. The data is stored in two different modes: spectrum mode and imaging mode (Figure S2). Spectrum mode is the conventional way of storing MSI data while imaging mode stores the MSI data as its transpose. The benefit of using the transpose when displaying an image is that the desired *m/z* values (and the corresponding mass range) can be read consecutively from the transpose into the internal memory, without having to read any other data.

Quantitation. The quantitation process uses data from a standard calibration curve. Each calibration standard applied on the tissue section is selected and defined as an annotated ROI. Quantitation can be performed based on the *m/z* intensity of the substance of interest or, if an internal standard has been used, the substance's normalized intensity. During the quantitation process, a tabulated list of the selected ROIs is displayed. The user specifies the quantity of each calibration standard in this table, and the software automatically creates a standard calibration curve that is displayed together with its slope, intercept, and regression coefficient. The distribution of the substance of interest can then be displayed in terms of its per-pixel abundance.

Visualization Methods. Four different interpolation methods can be used to display the measured intensity levels: nearest neighbor, bilinear, bilinear color blend, and bicubic interpolation. In addition, seven different rainbow scales are available along with red, green, blue, and black-white color

scales. The MSI layer can be viewed in combination with the underlying optical or histological image layer in one of three different ways. The first involves changing the opacity of the MSI layer. The second, preferred, method is to use intensity transparency, which makes the lowest intensity regions of the MSI layer transparent. The third method involves fusing the MSI layer with the optical and histological layer. Two sharpening fusion methods are available: an in-house developed image sharpening function, which enables edge detection based on the optical and histological layer, and Intensity-Hue-Saturation (IHS) image fusion. IHS image fusion is often used to fuse a high spatial resolution (gray scale) image with a second image that has a low spatial resolution (rainbow color scale) image.²⁵

Testing the Performance of Open-Access MSI Software with Large MSI Data Files. A software performance test was performed to compare msIQuant to other open access programs that can handle the imzML format. A computer equipped with an Intel i7 CPU, 8 GB of RAM, the Windows 7 SP1 64-bit operating system, a 1TB SSD hard drive, and an Intel HD Graphics 3000 graphics chipset with shared memory was used. The software programs used in the performance test were MALDIVision 2 (version 2.22, build 22206, Premier Biosoft, Palo Alto, CA), MSiReader (version 0.06, North Carolina State University, Raleigh, NC), TissueView (version 1.1, R 241, AB Sciex, Concord, ON, Canada), BioMap (version 3.8.0.4, Novartis Institute for BioMedical Research, Basel, Switzerland), Datacube Explorer (version 1.3.0.0, FOM Institute AMOLF, Amsterdam, Netherlands), and Omnispect (version 2.5, Appalachian State University, Boone, NC). The 64-bit versions of these programs were used in all cases. The software programs Mirion (Justus Liebig University Giessen, Giessen, Germany), SpectViewer (CEA-LIST, Palaiseau, France), and Quantinetix MALDI Imaging Software (ImaBiotech SAS, Loos, France) were not included in the benchmark test since they are not open access.

The test involved investigations of four parameters: ability to open large imzML data sets of different sizes, time required to load or convert imzML data sets, time required to load imzML data sets after conversion into the program's native data format (where possible), and time required to update an MSI image after selecting a new *m/z* value. Eight different imzML data sets with different properties were tested, including raw data generated by different mass analyzers and imzML data sets with different binary formats, mass spectra types, numbers of pixels, *m/z* ranges in the MSI spectra, and imzML binary file sizes. Time was measured using a stop watch.

The msIQuant software (available on the Internet at <http://www.maldi-msi.org>) was also compared to the flexImaging program (version 4.1, 64 bit, Bruker Daltonics), which is commonly used for MSI visualization (see the Supporting Information).

RESULTS AND DISCUSSION

We have developed a novel MSI quantitation software package that can handle data from different instrument types and manufacturers through the standardized open format imzML. Our previous software¹⁷ could only read data from one manufacturer (flexImaging, Bruker Daltonics), which uses the proprietary MSI data format XMAS. The functionalities of the earlier software included spectra processing, normalization, quantitation, and evaluation. However, the previous software lacked a user interface that would allow users to select ROI's

and display quantitation results graphically. In addition, the MSI data was text-based and required large amounts of disk space. The new software msIQuant has been completely rewritten to fulfill specifications defined by our group to meet the future demands of MSI experiments.

Fast Access of Large MSI Data Set without Data Reduction. An important factor when evaluating MSI data is the time needed to load a data set. MSI data tend to grow in size as newer instruments offer higher spatial and mass resolutions. The bigger the data set, the longer it takes to load the raw data. If the raw data is too large to be contained in the computer's primary memory, the conventional strategy is to perform data reduction and store the reduced data so that it can be loaded quickly when it is accessed next.

Other MSI software has managed the processing and accessing of large data sets in different ways. For example, the OpenMSI software package is using an approach called "chunking" of data to accelerate the access of selective data.²⁶ The chunking process splits the data into multiple independent subparts, which are stored separately in the data file, instead of typically storing and processing the MSI data one spectrum at a time.

Here we have approached the problem of rapidly accessing large data sets in a different way. An msIQuant data set consists of both MSI spectra and the corresponding MSI spectra transpose in two separate files. This makes it possible to quickly read a single spectrum from the MSI spectra files and to quickly read a single m/z channel from the MSI spectra transpose file (Figure S2).

Instrument- and Manufacturer-Independence. The msIQuant MSI data format contains information about the entire MSI experiment including raw data, normalization factors, spatial information, biological information, ROI data, and spectra processing parameters. As mentioned above, msIQuant data is created from data stored in the open access MSI data format, imzML. Specifically, the binary component of the imzML data is converted into continuous profile data to avoid further recalculation or conversion of the data after it has been read into the memory.

Figure 1 shows three images acquired with MSI instruments from three different manufacturers (Waters Corp., Bruker Daltonics, and Thermo Scientific), with different mass analyzers (TOF, FTICR, and orbitrap). The MS instruments used DESI²⁷ and MALDI ion sources, but other types of ion sources such as secondary ion mass spectrometry (SIMS) or nanospray desorption electrospray ionization (nano-DESI) can also be used because the conversion of MSI data to imzML format is independent of the ion source type.

Spectra Processing. Depending on the type of mass analyzer used for the MSI experiments, the spectra may require processing prior to analysis. The parameter that affects the quality of the processed image the most is baseline subtraction. The mass analyzer that needs baseline subtraction in general is the TOF analyzer. Mass analyzers such as FTICR and Orbitrap generate by default a baseline close to zero. The spectra processing functions available in msIQuant include baseline correction, baseline subtraction, baseline denoising, Savitzky-Golay smoothing,²⁸ mass recalibration, and automatic spectra alignment. The two most important processing methods for the production of accurate images are baseline subtraction and spectra alignment. Baseline subtraction increases the accuracy of the S/N ratio determination. Spectra alignment can reduce the effects of mass shifts that might occur during an MSI

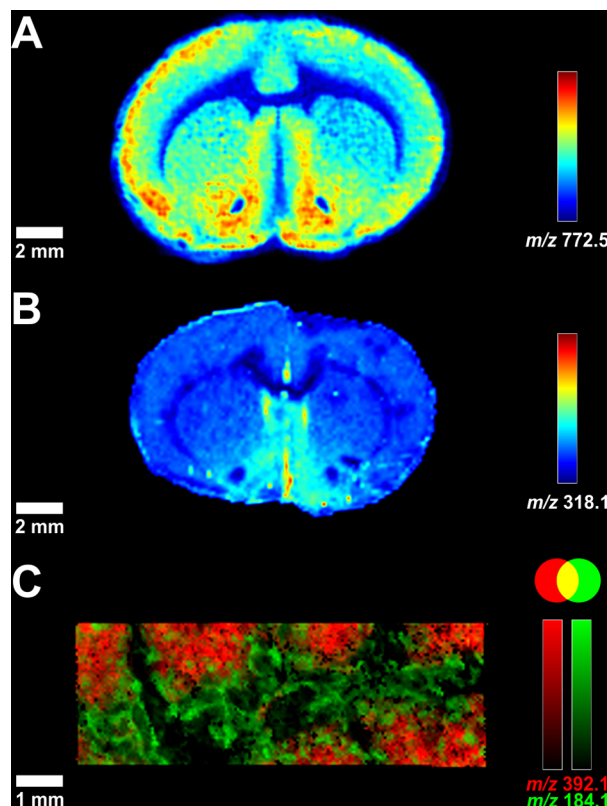


Figure 1. Ion images displayed by msIQuant generated by different MSI ion sources and instrument types. (A) A coronal rat brain tissue section displaying dipalmitoylphosphatidylcholine²⁹ (DPPC) $[M+K]^+$, m/z 772.5 at a spatial distribution of 150 μm . The image was generated with a DESI source (2D Source, Prosolia) coupled to a Q-TOF instrument (Synapt G2si, Waters Corp.). (B) A coronal rat brain tissue section displaying GABA (derivatized with DPP-TFB), m/z 318.1 at spatial distribution of 150 μm . The image was generated with a MALDI FTICR mass analyzer (SolariX FTMS, Bruker Daltonics). (C) A rat lung tissue section displaying tiotropium, m/z 392.1 (red) and the endogenous compound phosphocholine, m/z 184.1 (green) at a spatial distribution of 50 μm . The image was generated with a MALDI orbitrap instrument (LTQ Orbitrap, Thermo Scientific).

experiment. The algorithm used for spectra alignment extracts the strongest peaks from the average spectrum and uses them to align each individual spectrum. The alignment procedure is illustrated in Figure S3, which shows spectra for three different tissues and an average spectrum generated from the three original spectra. Before alignment, the positions of the m/z 379.1 peaks in the original spectra (which correspond to the dimer of CHCA, $[M_2+H]^+$) differ from that of the average spectrum by 0.026 Da. After alignment, the difference is reduced to less than 0.001 Da.

Visualization Methods. Normalization factor data can be used to visualize the median normalization, TIC normalization, RMS normalization, and internal standard normalization. The median, TIC, and RMS normalizations are all calculated with respect to all ions in a mass spectrum. Internal standard normalization is defined in terms of the ratio of the intensity of a selected analyte ion to that of a corresponding internal standard ion. If an internal standard is used, internal standard normalization should be used preferentially because it reduces the impact of ion suppression effects arising from tissue inhomogeneity and thus improves the level of pixel-to-pixel variation.¹⁷ msIQuant offers four different interpolation

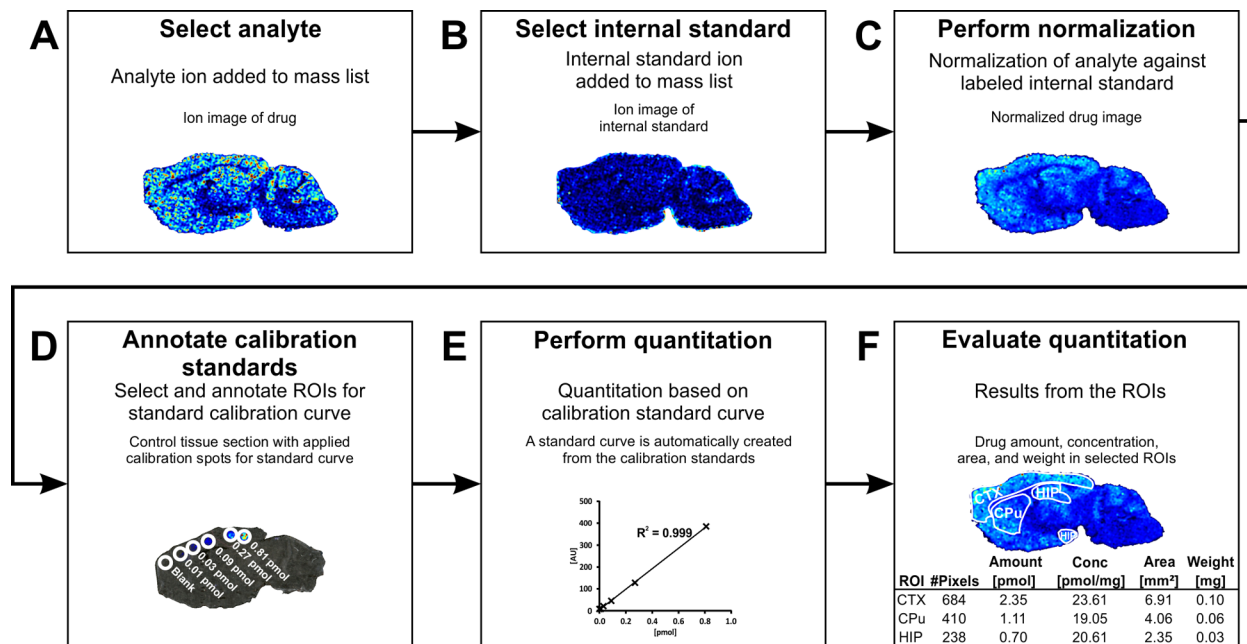


Figure 2. Quantitation protocol using msIQuant. The workflow for utilizing the software is exemplified by the analysis of a brain tissue section from an animal that had been treated with a drug. (A) Ion image of the drug from a sagittal mouse brain tissue section and (B) ion image of an isotopelabeled internal standard that was applied to the tissue section before matrix application. (C) The drug's ion intensity is then normalized in each pixel using the data for the internal standard. (D) A calibration standard curve is created by applying known quantities of the drug to separate regions of a control mouse brain tissue section and then selecting and annotating the corresponding ROIs. The internal standard is also applied to the tissue section before matrix application and the ion intensity is normalized in each pixel using the internal standard. (E) A calibration standard curve is automatically created using the data for the normalized calibration standards. (F) Three different brain regions, cortex (CTX), hippocampus (HIP), and caudate-putamen (CPu), are selected as ROIs, and the drug concentrations (pmol/mg) and amounts (pmol) in each are calculated using the evaluation function of msIQuant.

methods for displaying ion intensity levels (nearest neighbor, bilinear, bilinear color blend, and bicubic interpolation).^{29–32}

Creation of Regions-of-Interest in a Tissue Section.

One of the most important tools in MSI data processing is the creation of ROIs. Three different types of ROIs can be created in msIQuant: square, polygonal, or elliptical ROIs. Read-outs from these ROIs can subsequently be used for statistical analysis and to create calibration standard curves for quantitation. ROIs are created by accessing the image view, in which ROIs can be annotated and edited. In addition, it is possible to change their order or delete them if necessary. The information provided for each ROI includes the number of pixels it contains, the average intensity per pixel, and its area, perimeter, volume, and weight.

Quantitation. The quantitation procedure is exemplified in Figure 2, which shows the quantitation protocol for a sagittal mouse brain tissue sections from an animal treated with a drug. During sample preparation, a deuterated analogue of the drug was applied uniformly on top of the tissue sections as an internal standard. The drug's ion intensity is normalized against that of the internal standard to minimize sparse intensities in both dosed tissue and the control tissue section to which the calibration standards were applied. Three different regions of the dosed tissue, i.e. the cortex, caudate-putamen, and hippocampus, were selected, and the concentrations of the analyte were determined using the standard calibration curve. Since the tissue sections' thickness and density are both known, the measured concentrations can be expressed in units of mol per mg tissue.

We have earlier demonstrated that different normalization methods have a significant effect on the accuracy of the

standard calibration curves and the calculated tissue concentrations.¹⁷ Different normalization methods were investigated for the drug imipramine. Non-normalized data yielded the lowest linear correlation coefficient, whereas the highest correlation coefficient was obtained using the labeled (deuterated) internal standard normalization. There was also a difference in dynamic range between the normalization methods, the TIC normalization showed a limited dynamic range because of a logarithmic shaped standard curve compared to the internal standard normalization. By investigating imipramine concentrations in different regions of rat brains it was shown that the different normalization methods resulted in different drug levels and that the internal standard normalization generated the lowest relative standard deviations. This normalization approach also produced a lower deviation between neighboring pixels and compensated for false ion signals in tissue sections.¹⁷

The advantage of using a deuterated internal standard was further demonstrated by Chumbley et al.³³ to maximize quantitative reproducibility and accuracy by comparing MALDI-MSI quantitation with LC-MS/MS. The quantitative concentrations obtained from MALDI-MSI were comparable to LC-MS/MS results by >90% similarity.³³

Evaluation of Quantitative Data from ROIs. The evaluation function generates a list summarizing all the samples included in the current project and their ROIs, along with a numerical analysis of the selected ion distribution (Table S1). The information presented for each ROI includes the sum of its intensity counts, the sum of its intensity counts per unit area, per volume and per mass, the average intensity per pixel (including standard deviation and relative standard deviation),

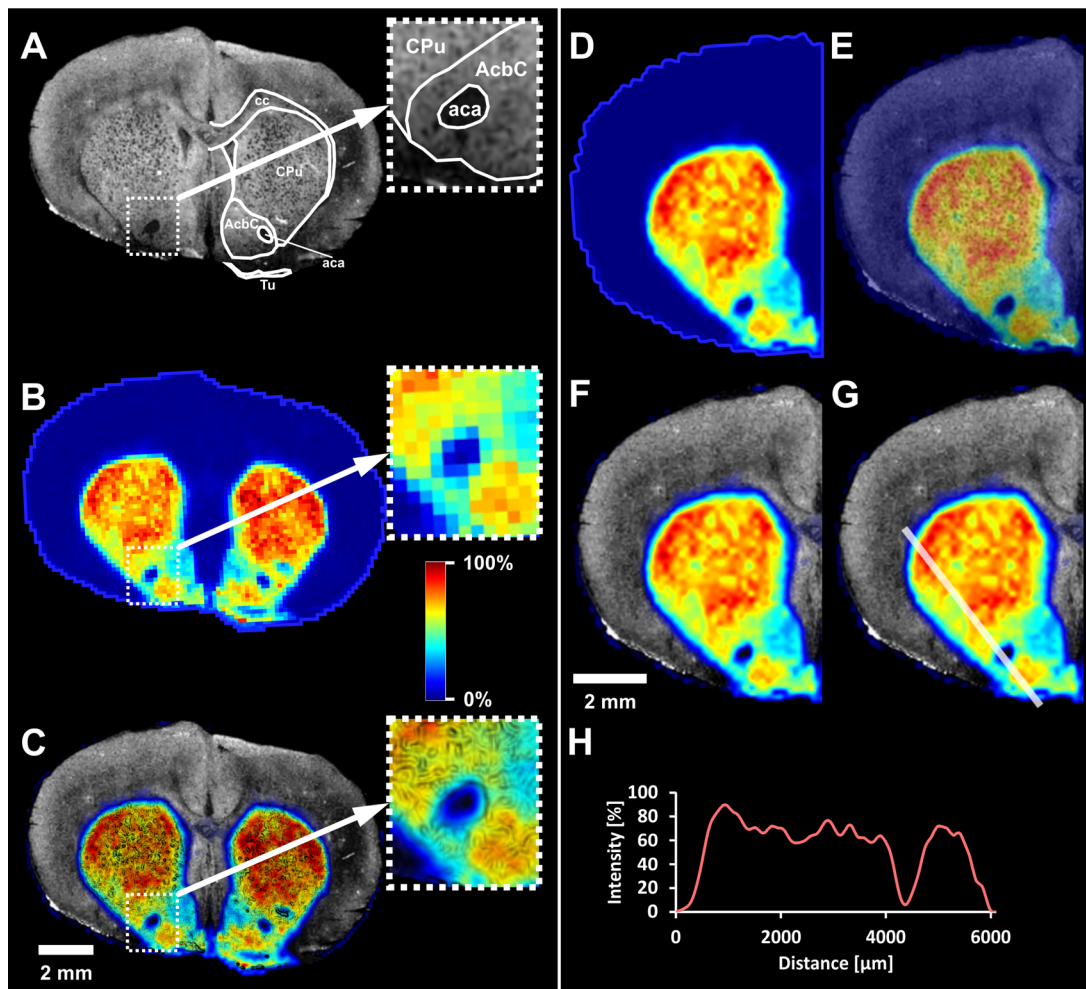


Figure 3. Low intensity transparency, profile intensity, and image fusion using msIQuant. (A) Optical image of a coronal rat brain tissue section displaying brain structures such as the corpus callosum (cc), striatum (caudate-putamen, CPu), nucleus accumbens, core (AcbC), anterior part of anterior commissure (aca), and olfactory tubercle (Tu) at 15 μm resolution. The magnified inset shows the aca, AcbC, and CPu. (B) Ion image of DA (m/z 368.165, derivatized DA with DPP-TFB) with nearest neighbor interpolation at 150 μm spatial resolution. (C) The DA image was sharpened with the image fusion function of msIQuant by using the optical image to display ion distribution at a spatial resolution smaller than that of the measured ion image. (D) An ion image showing the distribution of DA (derivatized DA with DPP-TFB) with bicubic interpolation at a spatial resolution of 150 μm . (E) The optical image is shown as the bottom layer, and the DA distribution is shown at 50% opacity in the top layer. (F) The optical image is shown in the bottom layer, and the DA ion distribution with low intensity transparency is shown on the top layer. The low intensity transparency makes it possible to preserve the brightness and contrast of both image layers. (G) The profile ion intensity of DA is selected from a defined area (width 200 μm and length 6082 μm), and (H) is displayed as a graph with the relative intensity of DA on the y -axis and the tissue length (μm) on the x -axis. The MS images were generated using a MALDI FTICR instrument (Bruker Daltonics).

the median intensity (as well as the Q1, Q3, minimum and maximum intensities), the number of measured pixels on the tissue section, and the ROI's area, perimeter, volume, and mass (see the *Supporting Information*).

Image Fusion and Profile Intensity Measurement.

Three features were implemented to enhance ion visualization: low intensity transparency, image sharpening, and IHS image fusion, which also can be used to sharpen MSI images. The image sharpening and IHS image fusion tools were implemented to fuse high-resolution histological or optical images with lower resolution MS images so that detailed information on molecular distributions could be correlated with specific tissue regions. The image sharpening process is exemplified by the fusion of an ion intensity image showing the distribution of dopamine at a pixel resolution of 150 μm with an optical image of the corresponding tissue section taken at a 15 μm pixel resolution (Figure 3A-C). The fused image

shows ion intensities at per pixel resolutions down to 15 μm . The image-sharpening algorithm incorporates edge detection based on the high-resolution histological or optical image into the fused image to emphasize structures visible in the high-resolution image.

The implementation of low intensity transparency enables better visualization of a fused image's intensity dynamics (Figure 3D-F). Regions of high intensity are completely opaque, while regions with intensities below 15% of the maximum are increasingly transparent. This enhances the visibility of the underlying histological and/or optical image. Without the low intensity transparency function, it is difficult to differentiate intensities close to zero. Low intensity transparency is required to achieve correct color rendering with respect to both the ion intensity and the optical image.

In addition, a profile ion intensity measurement was implemented to enable visualization of intensities for selected

Table 1. Comparison of Seven Different MSI Software Packages That Can Open Data in the imzML Format^a

A																					
file size	mass analyzer		binary format			spectrum type			no. of pixels			<i>m/z</i> range									
4.3 MB	FTICR		processed			centroid			27125			125.0–175.1									
10.7 MB	FTICR		processed			profile			5768			369.0–370.0									
18.5 MB	FTICR		continuous			profile			16200			225.0–249.9									
351 MB	TOF/TOF		continuous			profile			2871			159.8–1000.1									
2.5 GB	TOF/TOF		processed			profile			2871			159.8–1000.1									
2.9 GB	TOF/TOF		continuous			profile			99011			140.0–1157.7									
9.0 GB	Q-TOF		processed			profile			19370			100.0–999.9									
102 GB	TOF/TOF		processed			profile			99011			140.0–1157.7									
B																					
MALDIVision			MSiReader			TissueView			BioMap			Datacube Explorer									
file size	I	II	III	I	II	III	I	II	I	II	III	I	II	III							
4.3 MB	12	1	4.3	29	1.5	1	cannot open		1	1	0.01	cannot open	27	0.5	0.1						
10.7 MB	2	1	0.6	9	2.5	0.05	cannot open		5	-	0.05	2	0.5	0.01	2	-	3	10	0.5	0.05	
18.5 MB	2	1	2.1	18	3	0.6	8	-	0.1	8	-	0.1	2	0.5	0.01	cannot open			10	0.5	0.1
351 MB	5	1	2.1	10	5.5	0.6	cannot open		cannot open	10	2	0.01	cannot open	5	0.5	0.05					
2.5 GB	40	1	2.1	24	5.5	1.3	cannot open		cannot open	54	16	0.01	cannot open	54	0.5	0.05					
2.9 GB	cannot open			cannot open			cannot open		cannot open	cannot open		cannot open	cannot open	78	2.5	1.6					
9.0 GB	cannot open			571	720	181	cannot open		cannot open	cannot open		cannot open	cannot open	1201	1	0.1					
102 GB	cannot open			cannot open			cannot open		cannot open	cannot open		cannot open	cannot open	7401	2.5	1.6					

^aA) The software packages were tested using eight different imzML files that were generated with different mass analyzers, different binary file sizes, binary formats, mass spectrum types, numbers of pixels, and *m/z* ranges. B) Four different parameters were tested: ability to open the imzML data set, time required to load or convert the imzML data set, time required to load the data set after conversion into the program's native format, and time required to update an MSI image after selecting a new *m/z* value. I) Time (s) required to open or convert imzML file; II) time (s) required to open own data format, III) time (s) to update an image after selecting a *m/z* value.

ions along a predefined line along a tissue section with a set width (**Figure 3G–H**). The intensities can be copied to the clipboard and may be pasted into a spreadsheet, where the values can be plotted to retrieve information on both the ion intensities and measured distances.

Open Access MSI Software Performance Test of Large MSI Data Files. A software performance test was designed to measure the time required to create an image from imzML data or MSI data converted from imzML data. The purpose of the test was to compare the MSI data visualization performance of msIQuant to that of other software packages that use imzML format as input data. The tests consisted of eight imzML files with binary file sizes ranging from 4.3 MB to 102 GB and with different properties (see **Table 1a**). Six open access MSI software programs were evaluated alongside msIQuant. The performance tests (**Table 1b**) were divided into the following: ability to open the binary imzML data file, the time required to load or convert the imzML files, the time required to load the program's native data format, and the time required to update the displayed MSI image when a new *m/z* value is selected. Only msIQuant could load the 2.9 GB and 102 GB MSI data sets, because their data files and pixel counts were too large for the other programs. Aside from msIQuant, only one software program (MSiReader) could load and visualize the 9.0 GB file; MSiReader succeeded in this case because the number of pixels was lower than in the 2.9 GB and the 102 GB data files (see **Table 1**). Datacube Explorer can normally only open data files of less than 2 GB. However, this program successfully opened the 2.5 GB MSI data set because its binary data file contained redundant data on the *m/z* array and so the true size of the data set was only 1.2 GB. Datacube Explorer was also able to visualize the 2.9, 9.0, and 102 GB MSI files if their data was reduced to no more than 2 GB by reducing the image size (the number of pixels), the *m/z* range, or the number of *m/z*

channels by binning. Only msIQuant was able to convert all of the tested imzML data files and open them without data reduction.

The small data files (4.3 MB–2.5 GB) in the programs' native data formats (MALDIVision 2, MSiReader, and Datacube Explorer) were loaded quite quickly, in 0.5 to 14.5 s. However, when MSiReader opened the 9.0 GB MSI file after conversion into its native format, it took 720 s (12 min) to load, and 181 s was required to update the screen every time a new *m/z* value was selected. Conversely, msIQuant opened the same MSI files in 1 s and updated the computer screen in 0.1 s when a new *m/z* value was selected.

A comparative analysis of flexImaging (Bruker Daltonics) and msIQuant (**Table S2**) showed that the time required to create a reduced data set with flexImaging was comparable to that for the creation of an msIQuant data set from imzML data, but the msIQuant data was opened over 10 times more quickly than the reduced data set in flexImaging. That is, msIQuant can open nonreduced data set, whereas flexImaging needs to reduce its data size.

CONCLUSION

We have created a new MSI software package, msIQuant, for qualitative and quantitative analysis of drugs and endogenous compounds directly in tissue sections. The msIQuant software uses the open source MSI data format imzML to enable comparisons of data from different instrument manufacturers. The msIQuant software can analyze MSI data sets without any data reduction and without the need to load the complete MSI data set into the computer's internal memory. In addition, it offers four different interpolation methods, four different normalization methods, 11 built-in color scales for displaying ion intensities, low intensity transparency capabilities, and an

image fusion function for more detailed visualization of MS imaging data. To facilitate measurement and evaluation of tissue samples, three different ROI types can be created to define tissue structures and regions. Informative metrics are generated for each ROI defined in this way, including its area, perimeter, volume, and density, as well as its distribution of the targeted ions in terms of their mean intensity, standard deviation, median intensity, first and third quartile intensities, and minimum and maximum intensities. All graphs, images, and evaluations generated with msIQuant can be exported for postprocessing.

■ ASSOCIATED CONTENT

Supporting Information

The Supporting Information is available free of charge on the ACS Publications website at DOI: [10.1021/acs.analchem.5b04603](https://doi.org/10.1021/acs.analchem.5b04603).

The msIQuant user views, data processing and evaluation, visualization methods, MSI software performance test of large MSI data files, fast access of large MSI dataset without data reduction, evaluation of quantitative data from ROIs, Table S1 and S2, Figure S1, S2 and S3 ([PDF](#))

■ AUTHOR INFORMATION

Corresponding Author

*Phone: 46-70-167 9334. E-mail: per.andren@farmbio.uu.se.

Author Contributions

The study and manuscript was written and carried out through contributions of all authors. All authors approved the final version of the manuscript.

Notes

The authors declare no competing financial interest.

■ ACKNOWLEDGMENTS

We thank Per Svenningsson of the Karolinska Institute, Stockholm, Sweden for the supply of brain tissue sections, Philippa Hart and Emmanuelle Claude of Waters Corp., Manchester, UK for generating the DESI MS image (**Figure 1A**), and Matthias Witt of Bruker Daltonics, Bremen, Germany for generating the FTICR image (**Figure 3**). This work was supported by The Swedish Research Council (Medicine and Health #2013-3105, Natural and Engineering Science #2014-6215, Research Infrastructure #2009-6050) and National Institution of Drug Abuse (NIDA), grant R21 DA027548-01.

■ REFERENCES

- (1) Caprioli, R. M.; Farmer, T. B.; Gile, J. *Anal. Chem.* **1997**, *69*, 4751–4760.
- (2) Khatib-Shahidi, S.; Andersson, M.; Herman, J. L.; Gillespie, T. A.; Caprioli, R. M. *Anal. Chem.* **2006**, *78*, 6448–6456.
- (3) van Remoortere, A.; van Zeijl, R. J.; van den Oever, N.; Franck, J.; Longuespee, R.; Wisztorski, M.; Salzet, M.; Deelder, A. M.; Fournier, I.; McDonnell, L. A. *J. Am. Soc. Mass Spectrom.* **2010**, *21*, 1922–1929.
- (4) Skold, K.; Svensson, M.; Nilsson, A.; Zhang, X.; Nydahl, K.; Caprioli, R. M.; Svenningsson, P.; Andren, P. E. *J. Proteome Res.* **2006**, *5*, 262–269.
- (5) Jackson, S. N.; Ugarov, M.; Egan, T.; Post, J. D.; Langlais, D.; Albert Schultz, J.; Woods, A. S. *J. Mass Spectrom.* **2007**, *42*, 1093–1098.
- (6) Shariatgorji, M.; Nilsson, A.; Goodwin, R. J.; Kallback, P.; Schintu, N.; Zhang, X.; Crossman, A. R.; Bezard, E.; Svenningsson, P.; Andren, P. E. *Neuron* **2014**, *84*, 697–707.
- (7) Stoeckli, M.; Chaurand, P.; Hallahan, D. E.; Caprioli, R. M. *Nat. Med.* **2001**, *7*, 493–496.
- (8) Prideaux, B.; Dartois, V.; Staab, D.; Weiner, D. M.; Goh, A.; Via, L. E.; Barry, C. E., III; Stoeckli, M. *Anal. Chem.* **2011**, *83*, 2112–2118.
- (9) Biomedical Imaging Resource, Mayo Clinic, Rochester, MN, 1998. <https://rportal.mayo.edu/bir/ANALYZE75.pdf>.
- (10) Rompp, A.; Schramm, T.; Hester, A.; Klinkert, I.; Both, J. P.; Heeren, R. M.; Stockli, M.; Spengler, B. *Methods Mol. Biol.* **2011**, *696*, 205–224.
- (11) Rausch, M.; Stoeckli, M. 2000; pp BioMap. http://maldi-msi.org/index.php?option=com_content&view=article&id=14&Itemid=32 (accessed Mar 1, 2016).
- (12) Klinkert, I.; Chughtai, K.; Ellis, S. R.; Heeren, R. M. A. *Int. J. Mass Spectrom.* **2014**, *362*, 40–47.
- (13) Parry, R. M.; Galhena, A. S.; Gamage, C. M.; Bennett, R. V.; Wang, M. D.; Fernandez, F. M. *J. Am. Soc. Mass Spectrom.* **2013**, *24*, 646–649.
- (14) Paschke, C.; Leisner, A.; Hester, A.; Maass, K.; Guenther, S.; Bouschen, W.; Spengler, B. *J. Am. Soc. Mass Spectrom.* **2013**, *24*, 1296–1306.
- (15) Robichaud, G.; Garrard, K. P.; Barry, J. A.; Muddiman, D. C. *J. Am. Soc. Mass Spectrom.* **2013**, *24*, 718–721.
- (16) Both, J. P. 2011; pp SpectViewer (CEA). http://www.maldi-msi.org/index.php?option=com_content&view=article&id=313&Itemid=100 (accessed Mar 1, 2016).
- (17) Kallback, P.; Shariatgorji, M.; Nilsson, A.; Andren, P. E. *J. Proteomics* **2012**, *75*, 4941–4951.
- (18) Porta, T.; Lesur, A.; Varesio, E.; Hopfgartner, G. *Anal. Bioanal. Chem.* **2015**, *407*, 2177–2187.
- (19) Pirman, D. A.; Yost, R. A. *Anal. Chem.* **2011**, *83*, 8575–8581.
- (20) Pirman, D. A.; Reich, R. F.; Kiss, A.; Heeren, R. M.; Yost, R. A. *Anal. Chem.* **2013**, *85*, 1081–1089.
- (21) Pirman, D. A.; Kiss, A.; Heeren, R. M.; Yost, R. A. *Anal. Chem.* **2013**, *85*, 1090–1096.
- (22) Nilsson, A.; Fehniger, T. E.; Gustavsson, L.; Andersson, M.; Kenne, K.; Marko-Varga, G.; Andren, P. E. *PLoS One* **2010**, *5*, e11411.
- (23) Shariatgorji, M.; Nilsson, A.; Kallback, P.; Karlsson, O.; Zhang, X.; Svenningsson, P.; Andren, P. E. *J. Am. Soc. Mass Spectrom.* **2015**, *26*, 934–939.
- (24) Schramm, T.; Hester, A.; Klinkert, I.; Both, J. P.; Heeren, R. M.; Brunelle, A.; Laprevote, O.; Desbenoit, N.; Robbe, M. F.; Stoeckli, M.; Spengler, B.; Rompp, A. *J. Proteomics* **2012**, *75*, 5106–5110.
- (25) Choi, M. *Ieee T Geosci Remote* **2006**, *44*, 1672–1682.
- (26) Rubel, O.; Greiner, A.; Cholia, S.; Louie, K.; Bethel, E. W.; Northen, T. R.; Bowen, B. P. *Anal. Chem.* **2013**, *85*, 10354–10361.
- (27) Murphy, R. C.; Hankin, J. A.; Barkley, R. M. *J. Lipid Res.* **2009**, *50* (Suppl), S317–S322.
- (28) Savitzky, A.; Golay, M. J. E. *Anal. Chem.* **1964**, *36*, 1627–1639.
- (29) Sparvero, L. J.; Amoscato, A. A.; Dixon, C. E.; Long, J. B.; Kochanek, P. M.; Pitt, B. R.; Bayir, H.; Kagan, V. E. *Chem. Phys. Lipids* **2012**, *165*, 545–562.
- (30) Eberlin, L. S.; Liu, X.; Ferreira, C. R.; Santagata, S.; Agar, N. Y.; Cooks, R. G. *Anal. Chem.* **2011**, *83*, 8366–8371.
- (31) Rompp, A.; Both, J. P.; Brunelle, A.; Heeren, R. M.; Laprevote, O.; Prideaux, B.; Seyer, A.; Spengler, B.; Stoeckli, M.; Smith, D. F. *Anal. Bioanal. Chem.* **2015**, *407*, 2329–2335.
- (32) Guenther, S.; Rompp, A.; Kummer, W.; Spengler, B. *Int. J. Mass Spectrom.* **2011**, *305*, 228–237.
- (33) Chumbley, C. W.; Reyzer, M. L.; Allen, J. L.; Marriner, G. A.; Via, L. E.; Barry, C. E., 3rd; Caprioli, R. M. *Anal. Chem.* **2016**, *88*, 2392–2398.